AD-A113 589 NAVAL SURFACE WEAPONS CENTER SILVER SPRING MD F/G 20/7
STABILITY OF CHARGED BEAM PROPAGATION THROUGH A RELATIVISTIC HO--ETC(U)
SEP 81 H S UHM
UNCLASSIFIED NSWC/TR-81-391 SBI-AD-F500 004 NL

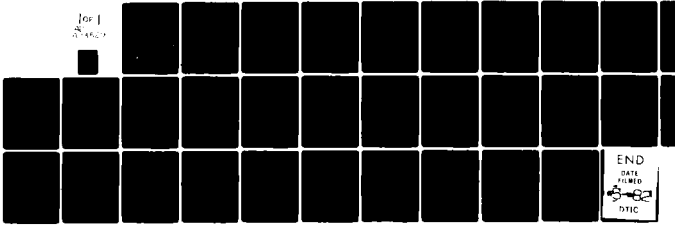

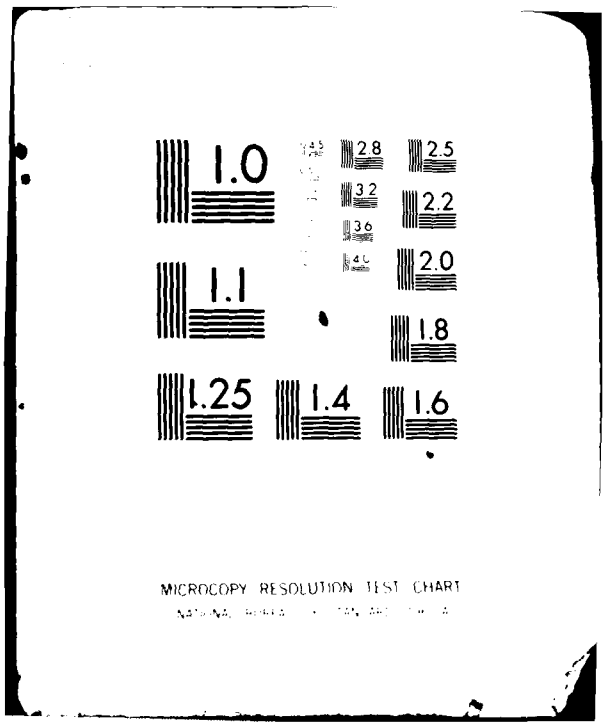
1.0
2.8
2.5
3.2
2.2
3.6
4.0
2.0
1.1
1.8
1.25
1.4
1.6
MICROCOPY RESOLUTION TEST CHART

NSWC TR 81-391

STABILITY OF CHARGED BEAM PROPAGATION THROUGH A RELATIVISTIC HOLLOW ELECTRON BEAM

BY HANS S. UHM

RESEARCH AND TECHNOLOGY DEPT.

SEPTEMBER 1981

NAVAL SURFACE WEAPONS CENTER

Dahlgren, Virginia 22448 • Silver Spring, Maryland 20910

UNCLASSIFIED

SECURITY CLASSIFICATION OF THIS PAGE (When Data Entered)

REPORT DOCUMENTATION PAGE		READ INSTRUCTIONS BEFORE COMPLETING FORM
1. REPORT NUMBER NSWC TR 81-391	2. GOVT ACCESSION NO. AD-A113 529	3. RECIPIENT'S CATALOG NUMBER
4. TITLE (and Subtitle) Stability of Charged Beam Propagation Through a Relativistic Hollow Electron Beam		5. TYPE OF REPORT & PERIOD COVERED Final 6. PERFORMING ORG. REPORT NUMBER
7. AUTHOR(s) Han S. Uhm		8. CONTRACT OR GRANT NUMBER(s)
9. PERFORMING ORGANIZATION NAME AND ADDRESS Naval Surface Weapons Center R41 White Oak, Silver Spring, Maryland 20910		10. PROGRAM ELEMENT, PROJECT, TASK AREA & WORK UNIT NUMBERS 61152N, ZR00001, ZR01109, 0
11. CONTROLLING OFFICE NAME AND ADDRESS		12. REPORT DATE September 1981 13. NUMBER OF PAGES 37
14. MONITORING AGENCY NAME & ADDRESS(if different from Controlling Office)		15. SECURITY CLASS. (of this report) UNCLASSIFIED 15a. DECLASSIFICATION/DOWNGRADING SCHEDULE

16. DISTRIBUTION STATEMENT (of this Report)

Approved for public release, distribution unlimited

17. DISTRIBUTION STATEMENT (of the abstract entered in Block 20, if different from Report)

18. SUPPLEMENTARY NOTES

19. KEY WORDS (Continue on reverse side if necessary and identify by block number)

Hollow Electron Beam
Charged Beam
Stability of E-Beam
Charged Particle Accelerator

20. ABSTRACT (Continue on reverse side if necessary and identify by block number)

Stability properties of a charged beam propagation through a relativistic hollow electron beam are investigated, in connection with present experimental applications in the collective particle accelerator. The stability analysis is carried out for long axial wavelength and low-frequency perturbations. A closed algebraic dispersion relation for coupled transverse oscillations is obtained for the solid and hollow beams with sharp-boundary density profiles. One of the most important features in the analysis is that the typical growth rate of the transverse oscillation is order of the hollow beam diocotron frequency $\omega_{\ldots}$

DD FORM 1 JAN 73 1473 EDITION OF 1 NOV 65 IS OBSOLETE
S/N 0102-014-6601

UNCLASSIFIED
SECURITY CLASSIFICATION OF THIS PAGE (When Data Entered)

thereby severely limiting the solid beam propagation through a relativistic hollow electron beam. However, for a solid beam with a small radius, the fundamental mode perturbation (i.e., the dipole oscillation) is the most unstable mode.

FOREWORD

Stability properties of a charged beam propagation through a relativistic hollow electron beam are investigated, in connection with present experimental applications in the collective particle accelerator. The stability analysis is carried out for long axial wavelength and low-frequency perturbations. A closed algebraic dispersion relation for coupled transverse oscillations is obtained for the solid and hollow beams with sharp-boundary density profiles. One of the most important features in the analysis is that the typical growth rate of the transverse oscillation is order of the hollow beam diocotron frequency ω_D, thereby severely limiting the solid beam propagation through a relativistic hollow electron beam. However, for a solid beam with a small radius, the fundamental mode perturbation (i.e., the dipole oscillation) is the most unstable mode.

Ira M Blatstein

IRA M. BLATSTEIN
By direction

CONTENTS

ILLUSTRATIONS

INTRODUCTION

In recent years, there have been numerous theoretical investigations of the equilibrium and stability properties[1,2] in intense relativistic hollow electron beams, motivated by a variety of applications, including microwave generation and amplification,[3,4] and collective effect acceleration[5-7] by relativistic hollow electron beams. Moreover, recent renewed interest in the equilibrium and stability properties[8,9] of charged particle beams propagating through a relativistic electron beam originates from several diverse research areas, including confinement and transport[10,11] of a nonneutral electron beam, the collective ion acceleration[12-14] and electron beam propagation[15,16] through a background plasma. In particular, the collective particle accelerator[5,6] is the acceleration of a charged particle beam propagating in a spatially modulated magnetic field. In this regard, this paper examines the equilibrium and stability properties of a solid charged beam propagating through an intense relativistic hollow electron beam, in connection with present experimental applications in the collective particle accelerator.

Investigation of the coupled transverse oscillation is carried out for an intense charged particle beam that is infinite in axial extent and propagates through a relativistic hollow electron beam. The stability analysis is calculated within the framework of a hybrid (Vlasov-fluid) model in which the hollow beam electrons are described as a macroscopic, cold fluid immersed in an axial magnetic field $B_0\hat{e}_z$, and the solid beam particles are described by the Vlasov equation. We assume that the radius of the solid beam R_s is less than the

inner radius R_1 of the hollow beam and that the hollow electron beam is tenuous. Moreover, it is further assumed that $\nu_s/\gamma_s << 1$, where the subscript denotes solid beam particles, ν_s is Budker's parameter, and $\gamma_s m_s c^2$ is the characteristic particle energy for the solid beam. Equilibrium properties and the basic assumptions are presented in Sec. II.

Stability analysis of coupled transverse oscillations is carried out in Sec. III for long axial wavelength and low-frequency perturbations. A closed algebraic dispersion relation [Eq. (28)] of the coupled transverse oscillation is obtained for the solid beam described by Eq. (6) and the hollow beam with density profile in Eq. (9). Equation (28) is one of the main results of this paper, and can be used to investigate stability properties for a broad range of system parameters of experimental interest. One of the most important features in this analysis is that the coupling between the hollow and solid beam modes is minimum whenever both beams have a same axial velocity. As a particular example, in the absence of either the solid beam or the hollow beam, we recover the previous results[1,17] from the dispersion relation in Eq. (28).

Making use of the dispersion relation in Eq. (28), stability properties for coupled transverse oscillations between the solid electron beam and the hollow electron beam is investigated in Sec. IV. Several points are noteworthy in the analysis in Sec. IV. First, for a solid beam satisfying $R_s << R_1$, the fundamental mode perturbation is the most unstable mode. Second, the typical growth rate of the transverse oscillation is a substantial fraction of the hollow beam diocotron frequency ω_D, thereby severely limiting the solid beam propagation through the hollow electron beam. The growth rate of the

conventional diocotron instability is much less than that of the coupled transverse oscillation for counter-streaming beams. However, the growth rate of instability reduces drastically with decreasing value of the density ratio $\hat{n}_s/\hat{n}_h$ of the solid beam to hollow beam. In this regard, a solid beam with a substantially reduced density can propagate through a counter-streaming hollow beam without a severe growth of unstable oscillations.

The ion resonance stability properties of a solid ion beam propagating through a hollow electron beam is investigated in Sec. V for a low density case. For a case of high density ion beam, we urge the reader to review the previous studies.[8,9] It is found from the analysis in Sec. V that the maximum growth rate of ion resonance instability is many times of the diocotron frequency. Moreover, the instability growth rate increases significantly as the solid beam radius R_s is increased.

THEORETICAL MODEL

The equilibrium configuration consists of an intense charged particle beam that is infinite in axial extent and propagates through a relativistic hollow electron beam with axial velocity $\beta_h c \hat{e}_z$. The axial velocity and radius of the solid beam are denoted by $\beta_s c\hat{e}_z$ and R_s, respectively. The inner and outer radii of the hollow beam is represented by R_1 and R_2, and this hollow beam is located inside a cylindrical conducting wall with radius R_c. For simplicity, we assume that the radius of the solid beam is less than the inner radius of the hollow beam, i.e., $R_s < R_1$. The applied axial magnetic field $B_0\hat{e}_z$ provides confinement of the equilibrium configuration in the radial direction. In the theoretical analysis, we introduce a cylindrical polar coordinate system (r,θ,z).

In order to make the analysis tractable, the following simplifying assumptions are made;

(a) The motion of the beam particles is predominantly in the axial direction, and that the transverse momentum is small in comparison with the characteristic axial momentum, i.e.,

$$p_r^2 + p_\theta^2 << p_z^2 , \tag{1}$$

where $\underset{\sim}{p} = (p_r, p_\theta, p_z)$ is the particle momentum in laboratory frame.

(b) The theoretical analysis is carried out for a tenuous hollow electron beam satisfying

$$\hat{\omega}_{ph}^2 << \omega_{ch}^2 , \tag{2}$$

where $\hat{\omega}_{ph}^2 = 4\pi e^2 \hat{n}_h/\gamma_h m$ is the plasma frequency-squared of hollow beam

electron, $\omega_{ch} = eB_0/\gamma_h mc$ is the hollow beam electron cyclotron frequency, and $\gamma_h = (1 - \beta_h^2)^{-1/2}$.

(c) It is further assumed that

$$\frac{\nu_s}{\gamma_s} = N_s \frac{Z_s^2 e^2}{m_s c^2} \frac{1}{\gamma_s} << 1 , \tag{3}$$

where s denotes solid beam particles, ν_s is Budker's parameter, $N_s = 2\pi \int_0^\infty dr\, r\, n_s^0(r)$ is the number of particles per unit axial length, $n_s^0(r)$ is the equilibrium particle density, -e is the electron charge, Z_s is the charge state of the solid beam particles, $\gamma_s m_s c^2$ is the characteristic particle energy for solid beam and c is the speed of light in vacuo.

The analysis is carried out within the framework of a hybrid (Vlasov-fluid) model in which the hollow beam electrons are described as macroscopic, cold fluid immersed in an axial magnetic field $B_0\hat{e}_z$ and the solid beam particles are described by the Vlasov equation. In this context, the equation of motion and the continuity equation for the hollow electron fluid can be expressed as

$$\left(\frac{\partial}{\partial t} + \underset{\sim}{V} \cdot \nabla\right)\gamma m \underset{\sim}{V} = -e\left(\underset{\sim}{E}_T + \frac{\underset{\sim}{V} \times \underset{\sim}{B}_T}{c}\right) , \tag{4}$$

$$\frac{\partial}{\partial t} n_h + \underset{\sim}{\nabla} \cdot (n_h \underset{\sim}{V}) = 0 , \tag{5}$$

where $\underset{\sim}{E}_T$ and $\underset{\sim}{B}_T$ are the electric and magnetic fields, respectively, n_h and $\underset{\sim}{V}$ are the density and mean velocity, respectively, of the hollow electron fluid element, m is the rest mass of electrons, and $\gamma(\underset{\sim}{x},t) = (1 - \underset{\sim}{V} \cdot \underset{\sim}{V}/c^2)^{-1/2}$. For present purposes, we assume that the equilibrium distribution function for the solid beam particle is of the form

$$f_s^0(\underset{\sim}{x},\underset{\sim}{p}) = (\hat{n}_s/2\pi\gamma_s m_s)\delta(H - \omega_s P_\theta - \hat{\gamma}_s m_s c^2) \times \delta(P_z - \gamma_s m_s \beta_s c) , \tag{6}$$

where $\hat{n}_s$ is the particle density at $r = 0$, $H = (m_s^2c^2 + c^2\underset{\sim}{p}^2)^{1/2} + e_s\phi_0(r)$ is the total energy, $P_\theta = r[p_\theta + (e_s/c)(rB_0/2)]$ is the canonical angular momentum, $P_z = p_z + (e_s/c)A_z^0(r)$ is the axial canonical momentum, e_s is the charge of the solid beam particles, $\phi_0(r)$ is the electrostatic potential for the equilibrium self-electric field, $A_z^0(r)$ is the axial component of vector potential for the azimuthal self-magnetic field, and ω_s, β_s, and $\hat{\gamma}_s$ are constants.

The density profile of the solid beam described by Eq. (6) is given by[9]

$$n_s^0(r) = \begin{cases} \hat{n}_s , & 0 \le r < R_s , \\ 0 , & \text{otherwise} , \end{cases} \tag{7}$$

where the radius of the solid beam is determined from $R_s^2 = \hat{v}_s^2/(\omega_s^+ - \omega_s)(\omega_s - \omega_s^-)$, the effective thermal velocity $\hat{v}_s$ is defined by $\hat{v}_s^2 = 2c^2(\hat{\gamma}_s - \gamma_s)/\gamma_s$,

$$\omega_s^\pm = -\frac{\varepsilon_s}{2}\omega_{cs}\left[1 \pm \left(1 - \frac{2\hat{\omega}_{ps}^2}{\gamma_s^2\omega_{cs}^2}\right)^{1/2}\right] , \tag{8}$$

are the laminar rotational frequencies in the fast (+) and slow (-) rotational equilibria, $\varepsilon_s = \text{sgn}(e_s)$, $\gamma_s = (1 - \beta_s^2)^{-1/2}$, and $\omega_{cs} = eZ_sB_0/\gamma_s m_s c$ and $\hat{\omega}_{ps} = (4\pi\hat{n}_s e_s^2/\gamma_s m_s)^{1/2}$ are the cyclotron and plasma frequencies, respectively, of the solid beam particles. Obviously, the equilibrium solution of the solid beam exist only for the rotational frequency ω_s satisfying $\omega_s^- < \omega_s < \omega_s^+$.

For present purposes, we also specialize to the sharp-boundary density profile of the hollow electron beam given by

$$n_h^0(r) = \begin{cases} \hat{n}_h = \text{const.}, & R_1 < r < R_2 , \\ 0 , & \text{otherwise} . \end{cases} \tag{9}$$

Since the mean velocity of an electron fluid element in the hollow electron beam is specified by $\underset{\sim}{V}_h^0(r) = V_{h\theta}^0(r)\hat{\underset{\sim}{e}}_\theta + \beta_h c\hat{\underset{\sim}{e}}_z$, the steady-state equation of motion in the azimuthal direction can be expressed as

$$\gamma_h m V_{h\theta}^{0\,2}(r)/r = e[E_r^0(r) - \beta_h B_\theta^0(r) + V_{h\theta}^0(r)B_0/c] , \tag{10}$$

from Eq. (4). In Eq. (10), $E_r^0(r)$ and $B_\theta^0(r)$ are the equilibrium radial electric and azimuthal magnetic fields, and $\hat{\underset{\sim}{e}}_\theta$ and $\hat{\underset{\sim}{e}}_z$ are unit vectors in the radial and azimuthal directions. Making use of the density profiles in Eqs. (7) and (9), it can be found that the field combination $E_r^0(r) - \beta_h B_\theta^0(r)$ in Eq. (10) is expressed as

$$\begin{aligned} E_r^0(r) - \beta_h B_\theta^0(r) &= -\frac{\partial}{\partial r}[\phi_0(r) - \beta_h A_z^0(r)] \\ &= 2\pi e_s \hat{n}_s (1 - \beta_s\beta_h)\frac{R_s^2}{r} - \frac{2\pi e\hat{n}_h}{\gamma_h^2}(r - R_1^2/r) , \end{aligned} \tag{11}$$

for $R_1 \le r \le R_2$. Substituting Eq. (11) into Eq. (10), and making use of Eqs. (2) and (3), we obtain the rotational frequency $\omega_h(r)$ of the hollow beam

$$\omega_h(r) = \omega_D\left(1 - \frac{R_1^2}{r^2} - \gamma_h^2\frac{\varepsilon_s\hat{n}_s Z_s}{\hat{n}_h}(1 - \beta_s\beta_h)\frac{R_s^2}{r^2}\right) , \tag{12}$$

where the diocotron frequency ω_D is defined by

$$\omega_D = \hat{\omega}_{ph}^2/2\gamma_h^2\omega_{ch} . \tag{13}$$

STABILITY ANALYSIS FOR COUPLED TRANSVERSE PERTURBATION

In this section, we make use of the linearized Vlasov-fluid and Maxwell equations to obtain the dispersion relation for coupled transverse oscillation of an intense charge beam propagating through a relativistic hollow electron beam. We adopt a normal-mode approach in which all perturbations are assumed to vary with time and space according to

$$\delta\Phi(\underset{\sim}{x},t) = \Phi(r)\exp\{i(\ell\theta+kz-\omega t)\} ,$$

where ω is the complex eigenfrequency with $\mathrm{Im}\omega > 0$, ℓ is the azimuthal harmonic number, and k is the axial wavenumber. The present stability analysis is carried out for long axial wavelength perturbations satisfying

$$k^2R_c^2 << (\ell^2 + 1) , \tag{14}$$

where R_c is the radius of the conducting wall. Moreover, the stability properties are investigated for low-frequency perturbation satisfying

$$|\omega R_c|^2/c^2 << (\ell^2 + 1) . \tag{15}$$

Within the context of Eqs. (14) and (15), it is straightforward to show that the Maxwell equations for perturbed fields can be approximated by[9]

$$\left(\frac{1}{r}\frac{\partial}{\partial r}\, r\, \frac{\partial}{\partial r} - \frac{\ell^2}{r^2}\right)\hat{\phi}(r) = -4\pi\hat{\rho}(r) , \tag{16}$$

and

$$\left(\frac{1}{r}\frac{\partial}{\partial r}\, r\,\frac{\partial}{\partial r} - \frac{\ell^2}{r^2}\right)\hat{A}(r) = -\frac{4\pi}{c}\,\hat{J}(r)\ , \tag{17}$$

where $\hat{\phi}(r)$ and $\hat{\rho}(r)$ are the perturbed electric potential and charge density, respectively, and $\hat{A}(r)$ and $\hat{J}(r)$ are the axial components of the perturbed vector potential and current density, respectively. Components of the perturbed fields can be expressed in terms of $\hat{\phi}(r)$ and $\hat{A}(r)$ as

$$\hat{E}_r(r) = -(\partial/\partial r)\hat{\phi}(r)\ , \quad \hat{E}_\theta(r) = -(i\ell/r)\hat{\phi}(r)\ ,$$

$$\hat{B}_\theta(r) = -(\partial/\partial r)\hat{A}(r)\ , \quad \hat{B}_r(r) = (i\ell/r)\hat{A}(r)\ , \tag{18}$$

$$\hat{E}_z(r) = -i[k\hat{\phi}(r) - (\omega/c)\hat{A}(r)]\ .$$

The perturbed charge $\hat{\rho}_h(r)$ and current $\hat{J}_h(r)$ densities contributed by the hollow electron beam can be calculated by linearizing the macroscopic fluid descriptions in Eqs. (4) and (5). Defining the effective perturbed hollow potential

$$\hat{\psi}_h(r) = \hat{\phi}(r) - \beta_h\hat{A}(r)\ , \tag{19}$$

and carrying out a straightforward algebraic manipulation, we obtain the hollow beam portion of the perturbed charge density[1]

$$\begin{aligned}\hat{\rho}_h(r) &= \hat{J}_h(r)/\beta_h c \\ &= \frac{\ell\hat{\psi}_h(r)}{4\pi r}\,\frac{1}{\omega_{ch}[\omega - k\beta_h c - \ell\omega_h(r)]}\,\frac{\partial}{\partial r}\,[\omega_{ph}^2(r)]\ ,\end{aligned} \tag{20}$$

where $\omega_{ph}^2(r) = 4\pi e^2 n_h^0(r)/\gamma_h m$ is the plasma frequency-squared of the hollow beam, and its derivative $(\partial/\partial r)\omega_{ph}^2(r)$ can be expressed as

$$\frac{\partial}{\partial r}\,\omega_{ph}^2(r) = \hat{\omega}_{ph}^2[\delta(r - R_1) - \delta(r - R_2)] ,$$

from Eq. (9). On the other hand, making use of the linearized Vlasov equation, the perturbed charge density $\hat{\rho}_s(r)$ contributed by the solid beam is given by[9]

$$\begin{aligned}\hat{\rho}_s(r) &= \hat{J}_s(r)/\beta_s c \\ &= -\frac{\ell\hat{\psi}_s(r)}{4\pi r}\,S\delta(r - R_s) ,\end{aligned} \tag{21}$$

where

$$\hat{\psi}_s(r) = \hat{\phi}(r) - \beta_s\hat{A}(r) , \tag{22}$$

is the effective perturbed solid potential, and

$$\begin{aligned}S = \frac{\hat{\omega}_{ps}^2 R_s^2}{\ell\hat{v}_s^2}\Bigg\{-1 + \left(\frac{\omega_s - \omega_s^+}{\omega_s^- - \omega_s^+}\right)^{\ell} \sum_{n=0}^{\ell} \frac{\ell!}{n!(\ell-n)!} \\ \times \frac{\omega - \ell\omega_s - k\beta_s c}{\omega - k\beta_s c - \ell\omega_s^- - n(\omega_s^+ - \omega_s^-)} \left(\frac{\omega_s^- - \omega_s}{\omega_s - \omega_s^+}\right)^n\Bigg\},\end{aligned} \tag{23}$$

is the effective susceptibility of the solid beam.

Substituting Eqs. (20) and (21) into Eqs. (16) and (17), and making use of the definitions of the effective potentials $\hat{\psi}_h(r)$ and $\hat{\psi}_s(r)$ give the coupled eigenvalue equations

$$\begin{aligned}\left(\frac{1}{r}\frac{\partial}{\partial r}\,r\,\frac{\partial}{\partial r} - \frac{\ell^2}{r^2}\right)\hat{\psi}_h(r) &= -\frac{\ell\hat{\psi}_h(r)}{\gamma_h^2 r}\,H(r)[\delta(r - R_1) - \delta(r - R_2)] \\ &\quad - \frac{\ell\hat{\psi}_s(r)}{r}\,(1 - \beta_s\beta_h)S\delta(r - R_s) ,\end{aligned} \tag{24}$$

and

$$\left(\frac{1}{r}\frac{\partial}{\partial r}\,r\,\frac{\partial}{\partial r} - \frac{\ell^2}{r^2}\right)\hat{\psi}_s(r) = -\frac{\ell\hat{\psi}_s(r)}{\gamma_s^2 r}\,S\delta(r - R_s)$$

$$- \frac{\ell\hat{\psi}_h(r)}{r} (1 - \beta_s\beta_h)H(r)[\delta(r - R_1) - \delta(r - R_2)] , \qquad (25)$$

where the effective susceptibility of the hollow beam is defined by

$$H(r) = \hat{\omega}_{ph}^2/\omega_{ch}[\omega - k\beta_h c - \ell\omega_h(r)] . \qquad (26)$$

It is evident that the right-hand sides of Eqs. (24) and (25) are equal to zero except at the surface of the beam boundaries ($r = R_s$, $r = R_1$, and $r = R_2$). Therefore, the eigenvalue equations (24) and (25) can be reduced to $r^{-1}(\partial/\partial r)(r\partial\hat{\psi}_j/\partial r) - (\ell^2/r^2)\hat{\psi}_j = 0$, except at $r = R_s$, $r = R_1$, and $r = R_2$. The eigenfunction satisfying Eqs. (24) and (25) are expressed as

$$\hat{\psi}_j(r) = \begin{cases} A_j r^{\ell} , & 0 < r < R_s , \\ B_j r^{\ell} + C_j r^{-\ell} , & R_s < r < R_1 , \\ D_j r^{\ell} + E_j r^{-\ell} , & R_1 < r < R_2 , \\ F_j(r^{\ell} - R_c^{2\ell} r^{-\ell}) , & R_2 < r < R_c , \end{cases} \qquad (27)$$

where the subscript $j = h$ and s denote the hollow and solid potentials, and the constants $A_j - F_j$ can be related by integrating Eq. (27) across the discontinuities at $r = R_s$, R_1, and R_2. After carrying out a straightforward algebraic manipulation, we obtain the dispersion relation for coupled transverse oscillation

$$\Gamma_h(\omega,k) \cdot \Gamma_s(\omega,k)$$

$$= \gamma_h^2\gamma_s^2(1 - \beta_s\beta_h)^2 \left(\frac{R_s}{R_1}\right)^{2\ell} \frac{S}{2\gamma_s^2} \left\{ \frac{H(R_1)}{2\gamma_h^2} \left(1 - \frac{R_1^{2\ell}}{R_c^{2\ell}}\right) \left[1 - \frac{R_1^{2\ell}}{R_c^{2\ell}} + \frac{H(R_2)}{2\gamma_h^2} \left(1 - \frac{R_1^{2\ell}}{R_2^{2\ell}}\right)\left(1 - \frac{R_2^{2\ell}}{R_c^{2\ell}}\right)\right] - \frac{H(R_2)}{2\gamma_h^2} \frac{R_1^{2\ell}}{R_2^{2\ell}} \left(1 - \frac{R_2^{2\ell}}{R_c^{2\ell}}\right)^2 \right\}, \qquad (28)$$

where the dielectric functions of the hollow and solid beams, $\Gamma_h(\omega,k)$ and $\Gamma_s(\omega,k)$, are defined by

$$\Gamma_h(\omega,k) = \frac{H(R_1)}{2\gamma_h^2}\left\{1 - \frac{R_1^{2\ell}}{R_c^{2\ell}} + \frac{H(R_2)}{2\gamma_h^2}\left(1 - \frac{R_1^{2\ell}}{R_2^{2\ell}}\right)\left(1 - \frac{R_2^{2\ell}}{R_c^{2\ell}}\right)\right\} - \frac{H(R_2)}{2\gamma_h^2}\left(1 - \frac{R_2^{2\ell}}{R_c^{2\ell}}\right) - 1 , \tag{29}$$

and

$$\Gamma_s(\omega,k) = \frac{S}{2\gamma_s^2}\left(1 - \frac{R_s^{2\ell}}{R_c^{2\ell}}\right) - 1 . \tag{30}$$

Equation (28) is the dispersion relation used in the remainder of this paper, and can be used to investigate stability properties for a broad range of system parameters of experimental interest.

In the limit of $S \to 0$, we recover the dispersion relation of the diocotron instability[1]

$$\Gamma_h(\omega,k) = 0 , \tag{31}$$

for a relativistic hollow beam from Eq. (28). On the other hand, in the absence of hollow beam (i.e., $H \to 0$), Eq. (28) reduces to

$$\Gamma_s(\omega,k) = 0 , \tag{32}$$

which is identical to the result obtained by Uhm and Davidson[17] for a relativistic nonneutral electron beam. A careful examination of the right-hand side of Eq. (28) shows that the coupling between the hollow and solid beam modes is minimum whenever $\beta_s = \beta_h$. Moreover, for a solid beam with its radius R_s satisfying $R_s << R_1$, the fundamental mode ($\ell = 1$) perturbation is the most unstable mode in the coupled transverse oscillations.

An important parameter that characterizes the importance of kinetic effects for solid beam is the ratio of the characteristic thermal Larmor radius ($\hat{r}_{Ls} = \hat{v}_s/\omega_{cs}$) to the beam radius R_s. Making use of the

beam radius definition in Eq. (7), it is straightforward to show that

$$\hat{r}_{Ls}^2/R_s^2 = (\omega_s - \omega_s^+)(\omega_s^- - \omega_s)/\omega_{cs}^2 ,$$

where $\omega_s^\pm$ is defined in Eq. (8), Evidently, the cold-fluid limit, where the beam motion is approximately laminar with $\hat{r}_{Ls}^2 << R_s^2$, corresponds to rotation velocities that satisfy $\omega_s \simeq \omega_s^\pm$. A careful examination of the expression for S shows that[18]

$$\lim_{\omega_s \to \omega_s^\pm} S(\omega,k) = \frac{\hat{\omega}_{ps}^2}{(\omega - k\beta_s c - \ell\omega_s^\pm)[(\omega - k\beta_s c - \ell\omega_s^\pm) + \epsilon_s\omega_{cs} + 2\omega_s^\pm]} . \tag{33}$$

Although the finite Larmor radius effects of the solid beam particles are important[18] on the stability properties, the numerical analysis of the dispersion relation in Eq. (28) is restricted to the cold particles characterized by $\hat{r}_{Ls}/R_s \to 0$. Moreover, in the remainder of this paper, we assume that the solid beam particles are in a slow rotational equilibrium, i.e., $\omega_s = \omega_s^-$.

STABILITY PROPERTIES OF A SOLID ELECTRON BEAM

In this section, we investigate the stability properties for coupled transverse oscillations between the solid electron beam and the hollow electron beam. Since the cyclotron frequency of the solid beam electrons is much higher than its rotation frequency

$$\omega_s = \omega_s^- \simeq \hat{\omega}_{ps}^2/2\gamma_s^2\omega_{cs} \ , \tag{34}$$

or the eigenfrequency (i.e., $\omega_{cs} >> \omega_s^-$ or $\omega_{cs} >> \omega$), the effective susceptibility $S(\omega,k)$ of the solid beam in Eq. (33) can be approximated by

$$S(\omega,k) = - \frac{\hat{\omega}_{ps}^2}{(\omega - k\beta_s c - \ell\omega_s^-)\omega_{cs}} \ . \tag{35}$$

Defining the normalized Doppler-shifted eigenfrequency Ω by

$$\Omega = (\omega - k\beta_s c)/\omega_D \ , \tag{36}$$

and substituting Eq. (35) into Eq. (28), we calculate the normalized growth rate $\Omega_i = \mathrm{Im}\Omega$ and Doppler-shifted real oscillation frequency $\Omega_r = \mathrm{Re}\Omega$ numerically from Eq. (28) for a broad range of system parameters, ℓ, β_h, β_s, $\hat{n}_s/\hat{n}_h$, R_s/R_c, R_1/R_c, and R_2/R_c. However, we emphasize that the normalized growth rate Ω_i calculated in this section is independent of the parameter $\hat{\omega}_{ph}^2/\omega_{ch}^2$.

Shown in Fig. 1 is plots of the normalized growth rate $\Omega_i = \mathrm{Im}\Omega$ versus kc/ω_D for $R_1/R_c = 0.857$, $R_2/R_c = 0.939$, $R_s/R_c = 0.2$, $\beta_h = 0.968$ (γ_h=4), $\ell = 1$, $\hat{n}_s/\hat{n}_h = 0.1$, and several values of β_s. For a small radius solid beam ($R_s/R_c = 0.2 << 1$) consistent with the present experiment,[19] the $\ell = 1$ perturbation is the most unstable mode. In these physical parameters, the growth rate of instability for a coupled transverse oscillation is a substantial fraction of the diocotron frequency ω_D, thereby severely limiting the solid beam propagation. The axial wavenumber

and the real oscillation frequency corresponding to the maximum growth rate of instability satisfy $|kc/\omega_D| \lesssim 1$ and $|\Omega_r| \approx 0.1$, respectively. However, we also note from Fig. 1 that small growth rate in range $0.5 < kc/\omega_D < 2$ is a residual influence of the familiar diocotron instability. Therefore, we conclude that the growth rate of the diocotron instability is much less than that of the coupled transverse oscillation for counter-streaming beams.

The dependence of stability properties on axial velocity of the solid beam is illustrated in Fig. 2, where the normalized maximum growth rate Ω_i^m is plotted versus β_s for the parameters identical to Fig. 1. The maximum growth rate of instability almost linearly reduces to zero as the value β_s increases from $\beta_s = -1$ to $\beta_s = \beta_h = 0.968$. In this regard, it is evident that the $\ell = 1$ mode perturbation is stable when the solid and hollow beams have a same axial velocity. This is consistent with the previous study.[2] Of considerable interest for experimental application is the stability behavior for specified values of β_h and β_s. Typical result is shown in Fig. 3 where the maximum growth rate Ω_i^m is plotted versus $\hat{n}_s/\hat{n}_h$ for $\beta_s = -0.943$ ($\gamma_s = 3$) and parameters otherwise identical to Fig. 1. Obviously from Fig. 3, the maximum growth rate of instability reduces drastically with decreasing value of the density ratio $\hat{n}_s/\hat{n}_h$. We therefore conclude that a solid beam with a substantial density reduction can propagate through a counter-streaming hollow beam, without a severe growth of unstable transverse oscillations.

ION RESONANCE INSTABILITY IN A HOLLOW ELECTRON BEAM

The ion resonance instability[18] is one of the fundamental instabilities that characterize a relativistic nonneutral plasma system with both ion and electron components. In this section, we investigate ion resonance stability properties of a solid ion beam propagating through a hollow relativistic electron beam. The stability analysis in this section is restricted to $R_s \leq R_1$ which requires a low density ion beam satisfying

$$2\hat{\omega}_{ps}^2 < \gamma_s^2\omega_{cs}^2 . \tag{37}$$

For the ion resonance instability in a high density ion beam with $2\hat{\omega}_{ps}^2 > \gamma_s^2\omega_{cs}^2$, we urge the reader to review the previous study.[9] Defining the normalized Doppler-shifted eigenfrequency Ω by $\Omega = (\omega - k\beta_s c)/\omega_D$ in Eq. (36), we have obtained the growth rate and real oscillation frequency numerically from Eq. (28) for a broad range of system parameters $\hat{\omega}_{ph}^2/\omega_{ch}^2$, R_s/R_c, β_s, and $\hat{n}_s/\hat{n}_h$. In this section, we summarize the essential features of the stability studies. The numerical analysis is restricted to the choice of parameters $\beta_h = 0.995$ ($\gamma_h = 10$), $\hat{\omega}_{ph}^2/\omega_{ch}^2 = 0.1$, $R_1/R_c = 0.857$, $R_2/R_c = 0.939$ and $m_s/m = 1836$ (proton beam).

The dependence of stability properties on axial wavenumber k is illustrated in Fig. 4, where (a) the normalized growth rate and (b) Doppler-shifted real oscillation frequency are plotted versus kc/ω_D for $R_s/R_c = 0.8$, $\beta_s = 0.1$, $\hat{n}_s/\hat{n}_h = 0.01$, and the azimuthal harmonic number $\ell = 1$ and 2. In Fig. 4(b), the real oscillation frequency is plotted only for the ranges of kc/ω_D corresponding to instability ($\mathrm{Im}\,\Omega > 0$). Several features are noteworthy in Fig. 4. First, the maximum growth rate of instability is many times of the diocotron frequency, thereby

severely limiting the ion beam propagation through a relativistic hollow electron beam. Second, as shown in Fig. 4(a), where $R_s/R_l = 1$, perturbations with azimuthal harmonic number $\ell \geq 2$ are the most unstable mode. Finally, we note from Fig. 4(a) that the growth rate of the diocotron instability in the range $kc/\omega_D \gtrsim 10$ is much less than that of the ion resonance instability. Shown in Fig. 5 are plots of the normalized growth rate versus kc/ω_D for $\ell = 1$, several values of β_s and parameters otherwise identical to Fig. 4. As expected, the growth rate of instability is a decreasing function of the parameter β_s.

In order to illustrate the dependence of stability properties on the solid beam radius, we present the normalized growth rate versus $\hat{n}_s/\hat{n}_h$ in Fig. 6 for several values of ℓ, and (a) $R_s/R_c = 0.8$ and (b) $R_s/R_c = 0.4$. It is evident from Fig. 6 that the instability growth rate increases significantly as the solid beam radius R_s is increased. Moreover, it is also noted from Fig. 6(b) that for small beam radius, the $\ell = 1$ mode is the most unstable mode. For example, the growth rate of the $\ell = 4$ perturbation in Fig. 6(b) is that of the typical diocotron instability. After a careful examination of Figs. 6(a) and (b), we finally note that for a specified value of $(\hat{n}_s/\hat{n}_h)(R_s/R_c)^2$ corresponding to the total ion current, the growth rate of the coupled transverse oscillation reduces considerably as the ion beam radius is decreased.

CONCLUSIONS

In this paper, we have investigated the stability properties of coupled transverse oscillations of a solid particle beam propagating through a relativistic hollow electron beam. The analysis was carried out within the framework of a hybrid (Vlasov-fluid) model in which the hollow beam electrons are described as a macroscopic cold fluid and the solid beam particles are described by Vlasov equation. Equilibrium properties and the basic assumptions were presented in Sec. II. Stability analysis of coupled transverse oscillations was carried out in Sec. III for long axial wavelength and low-frequency perturbations. A closed algebraic dispersion relation in Eq. (28) was obtained from the solid and hollow beams with sharp-boundary density profiles in Eqs. (7) and (9). One of the most important features in the analysis is that the coupling between the hollow and solid beam modes is minimum whenever both beams have a same axial velocity.

Stability properties for coupled transverse oscillations between the solid electron beam and the hollow electron beam was investigated in Sec. IV. We found that the typical growth rate of the transverse oscillation is a substantial fraction of the diocotron frequency ω_D, thereby severely limiting the solid beam propagation through the hollow electron beam. The growth rate of the conventional diocotron instability is much less than that of the coupled transverse oscillations for counter-streaming beams. Finally, the ion resonance stability properties of a solid ion beam was investigated in Sec. V for a low density case. It was found that the maximum growth rate of the ion resonance instability is many times of the diocotron frequency. Moreover, the instability growth rate increases significantly as the solid beam radius R_s is increased.

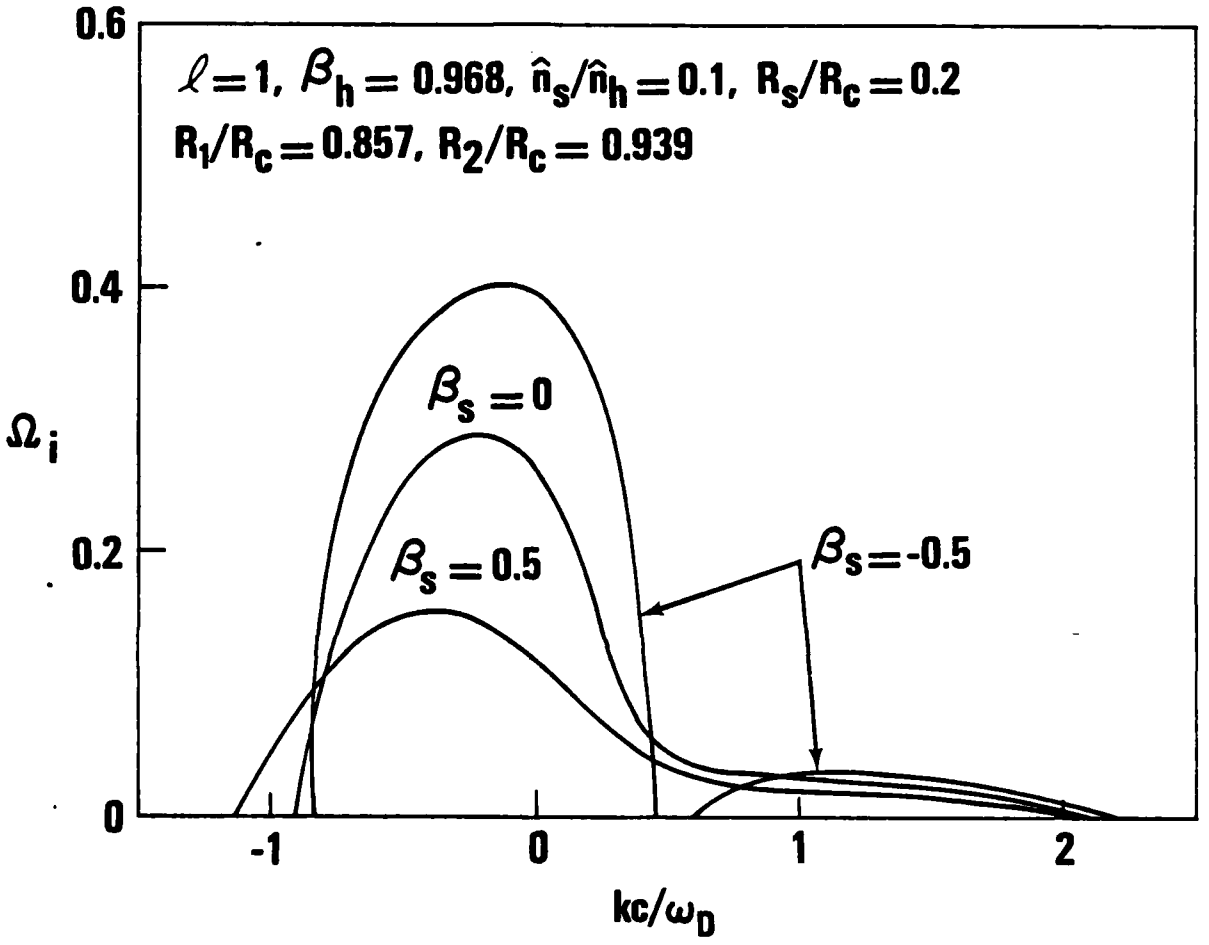

Fig. 1 Plot of normalized growth rate Ω_i versus kc/ω_D for electron-electron interaction, $R_1/R_c = 0.857$, $R_2/R_c = 0.939$, $R_s/R_c = 0.2$, $\beta_h = 0.968$, $\ell = 1$, $\hat{n}_s/\hat{n}_h = 0.1$, and several values of β_s

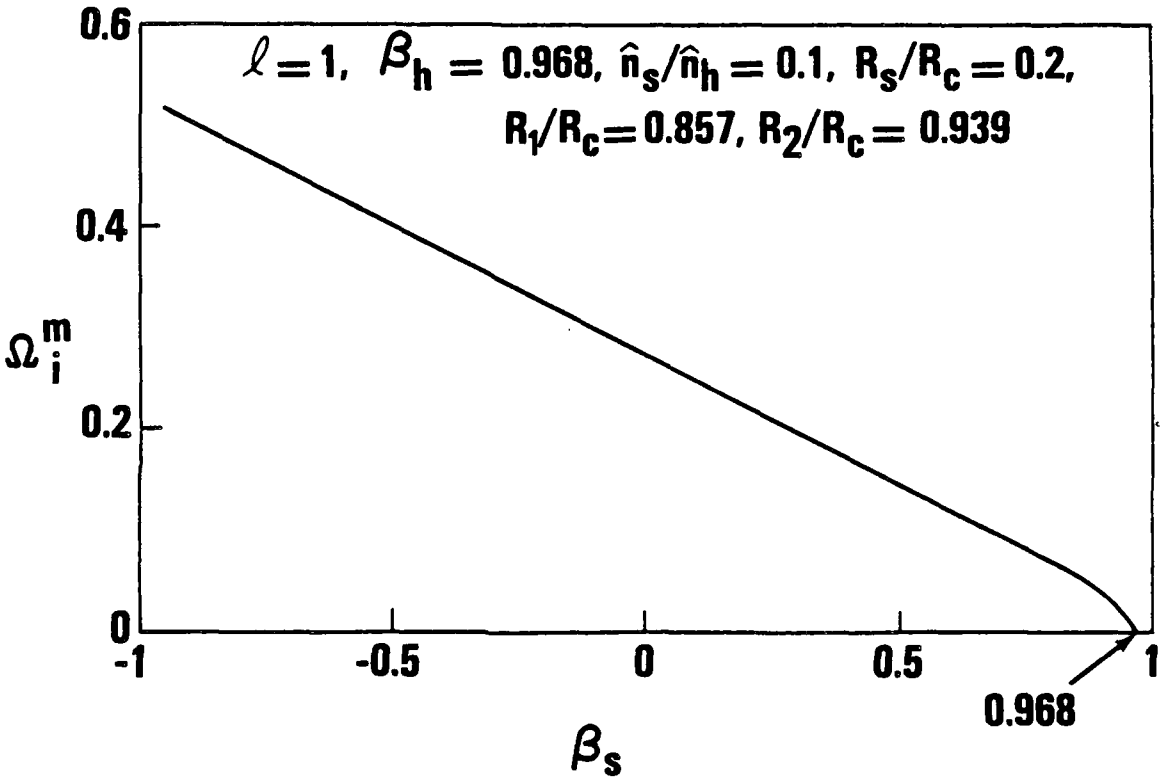

Fig. 2 Plot of normalized maximum growth rate Ω_i^m versus β_s for parameters identical to Fig. 1

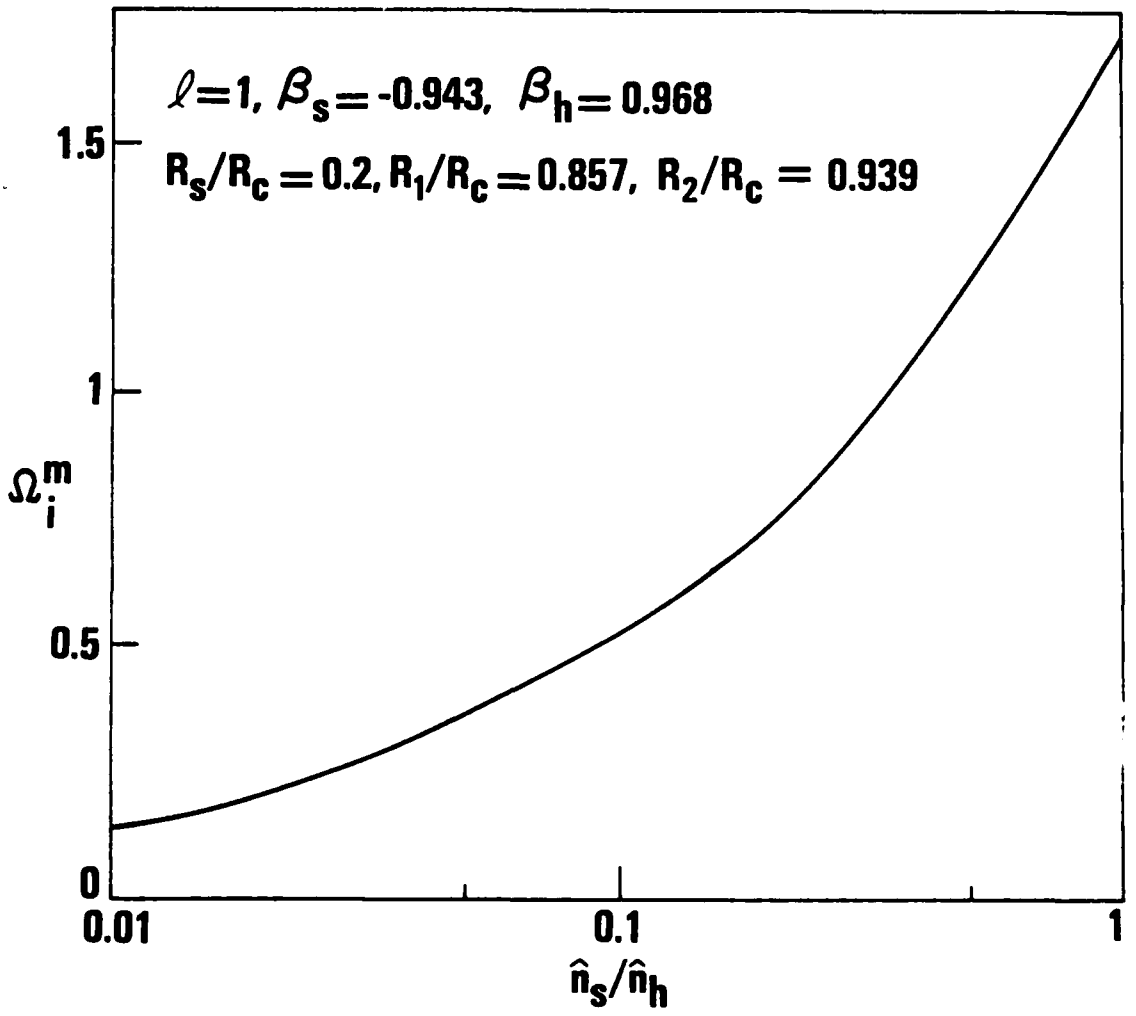

Fig. 3 Plot of normalized maximum growth rate Ω_i^m versus $\hat{n}_s/\hat{n}_h$ for β_s =-0.943 (γ_s = 3) and parameters otherwise identical to Fig 1

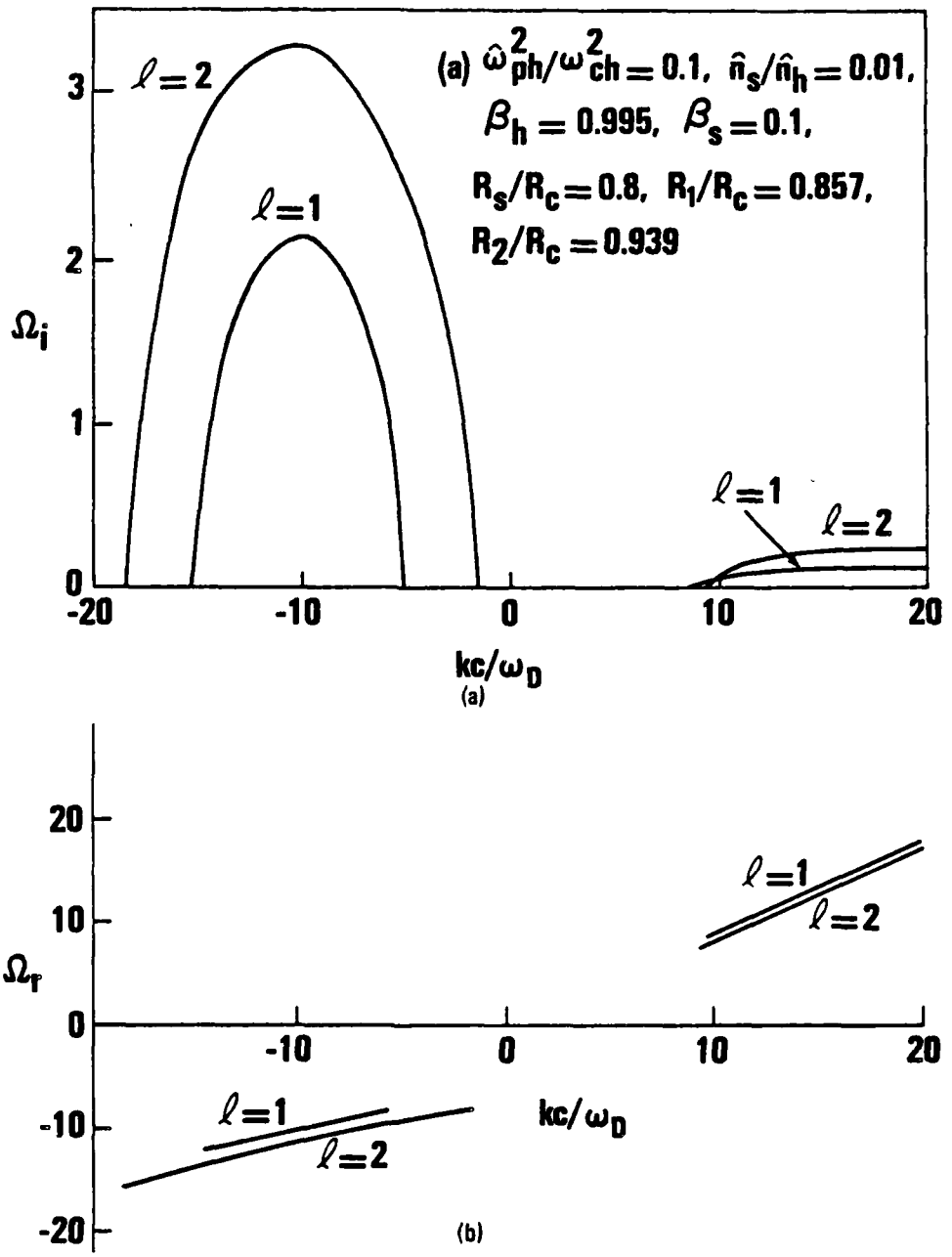

Fig. 4 Plot of (a) normalized growth rate Ω_i and (b) Doppler-shifted real oscillation frequency Ω_r versus kc/ω_D for proton-electron interaction, $\hat{\omega}^2_{ph}/\omega^2_{ch} = 0.1$, $R_1/R_c = 0.857$, $R_2/R_c = 0.939$, $\beta_h = 0.995$ ($\gamma_h = 10$), $R_s/R_c = 0.8$, $\beta_s = 0.1$, $\hat{n}_s/\hat{n}_h = 0.01$, and $\ell = 1$ and 2

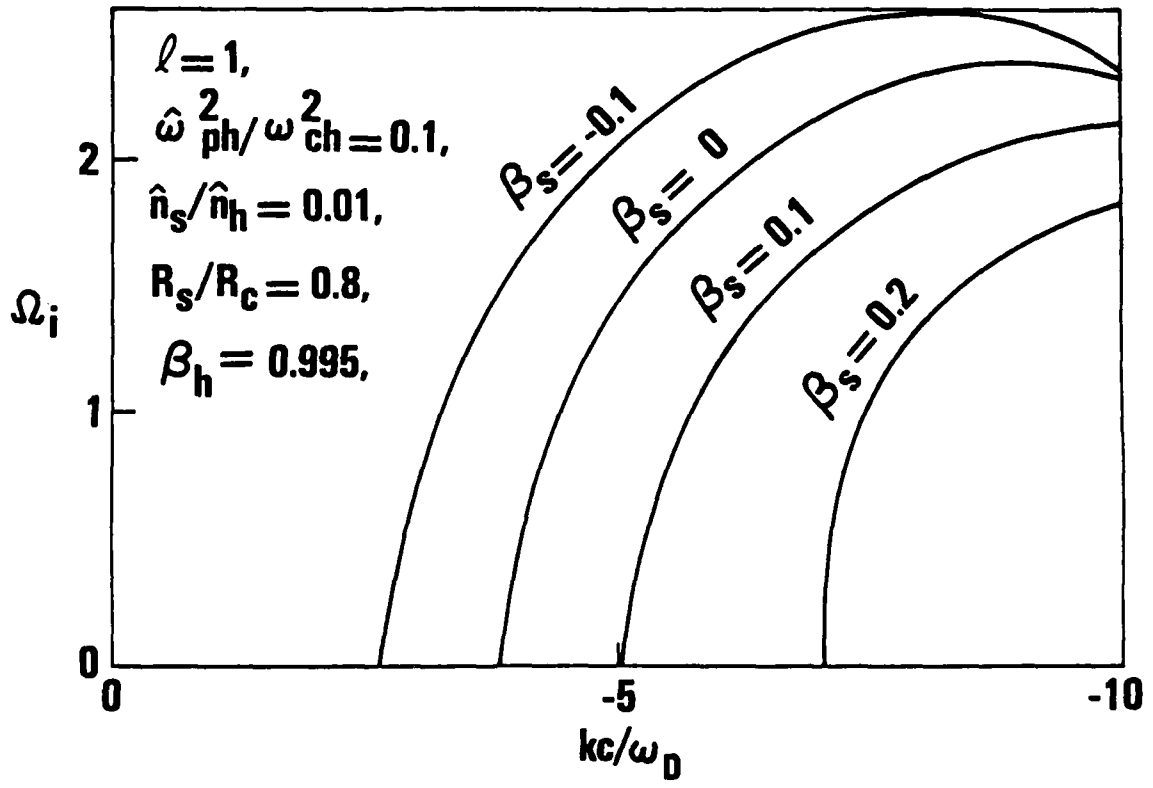

Fig. 5 Plot of normalized growth rate Ω_i versus kc/ω_D for $\ell = 1$, several values of β_s and parameters otherwise identical to Fig. 4

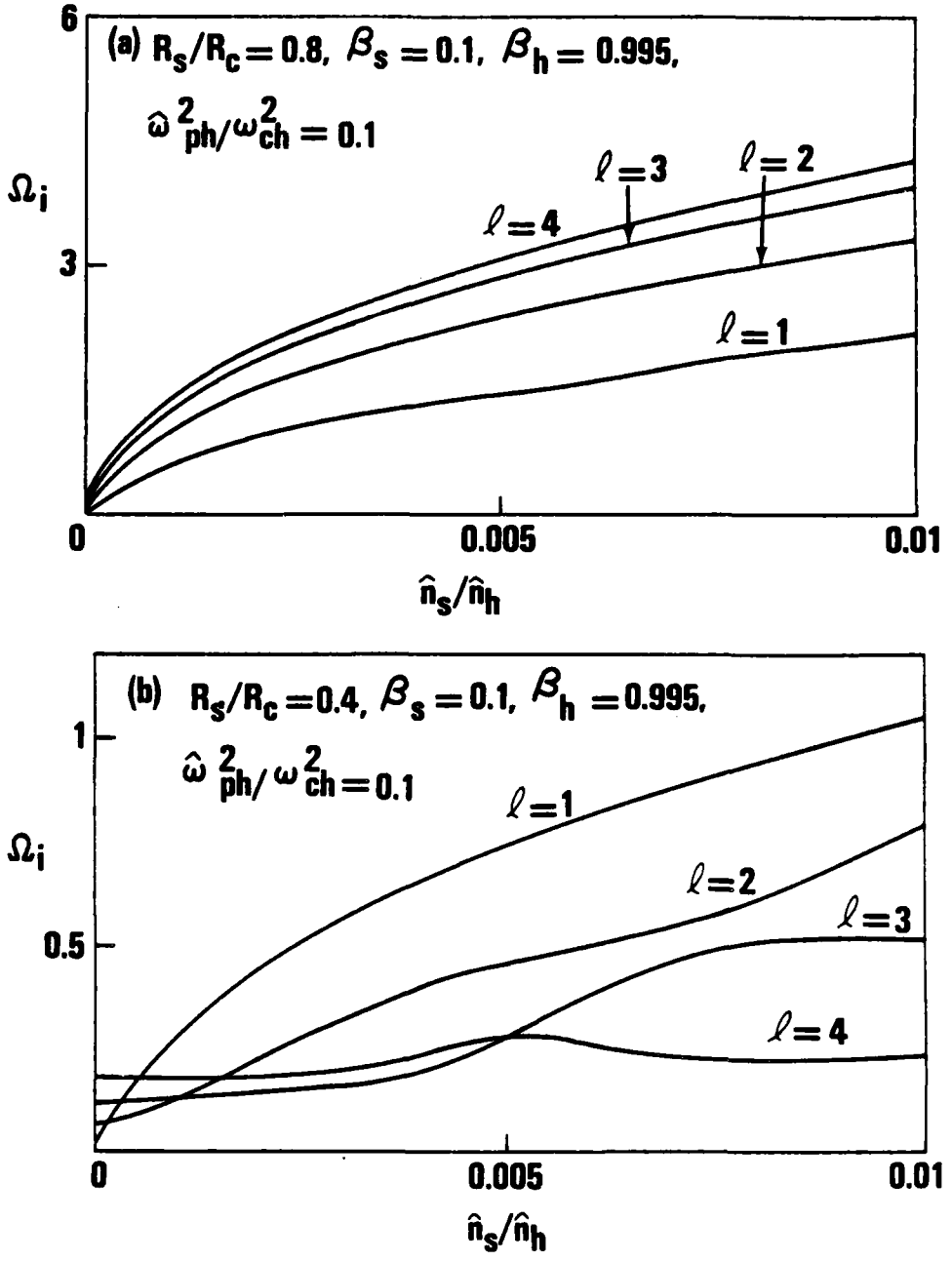

Fig. 6 Plot of normalized growth rate Ω_i versus $\hat{n}_s/\hat{n}_h$ for (a) $R_s/R_c = 0.8$, (b) $R_s/R_c = 0.4$, several values of ℓ, and parameters otherwise identical to Fig. 4

ACKNOWLEDGMENTS

It is a pleasure to acknowledge the benefit of useful discussions with Drs. M. Friedman and P. J. Palmadesso.

This research was supported by the Independent Research Fund at Naval Surface Weapons Center and by the Department of Defense Advanced Research Projects Agency.

REFERENCES

1. H. S. Uhm and J. G. Siambis, Phys. Fluids 22, 2377 (1979).
2. H. C. Chen and P. J. Palmadesso, Phys. Fluids 24, 357 (1981).
3. J. L. Hirschfield and V. L. Granatstein, IEEE Trans. Microwave Theory Tech. MTT-25, 528 (1977).
4. D. B. McDermott, T. C. Marshall, S. P. Schlesinger, R. K. Parker, and V. L. Granatstein, Phys. Rev. Lett. 41, 1368 (1978).
5. M. Friedman, In the Proc. of the Second Int. Topical Conf. on High Power Electron and Ion Beam Research and Technology, Ed. J. A. Nation and R. N. Sudan, (Cornell University, Ithaca, N. Y. 1977), p. 533.
6. M. Friedman, IEEE Trans. NS-26, 4186 (1979).
7. T. R. Lockner and M. Friedman, IEEE Trans. NS-26, 4237 (1979).
8. R. C. Davidson and H. S. Uhm, J. Appl. Phys. 51, 885 (1980).
9. H. S. Uhm and R. C. Davidson, Phys. Fluids 23, 813 (1980).
10. J. S. DeGassie and J. H. Malmberg, Phys. Rev. Lett. 39, 1078 (1977).
11. J. H. Malmberg and T. M. O'Neil, Phys. Rev. Lett. 39, 1334 (1977).
12. R. Adler, J. A. Nation, and V. Serlin, Phys. Fluids 24, 347 (1981).
13. E. Cornet, H. A. Davis, T. P. Starke, and W. W. Rienstra, to be submitted to Physics of Fluids (1981).
14. W. W. Destler, H. S. Uhm, H. Kim, and M. P. Reiser, J. Appl. Phys. 50, 3015 (1979).
15. C. A. Kapetanakos, Appl. Phys. Lett. 25, 481 (1974).
16. E. J. Lauer, R. J. Briggs, T. J. Fessendon, R. E. Hester, and E. P. Lee, Phys. Fluids 21, 1344 (1978).
17. H. S. Uhm and R. C. Davidson, Phys. Fluids 23, 1586 (1980).
18. R. C. Davidson and H. S. Uhm, Phys. Fluids 21, 60 (1978).
19. M. Friedman, private communication (1981).

DISTRIBUTION

	Copies
Commander	
Naval Research Laboratory	
Attn: Dr. Saeyoung Ahn	1
Dr. Wahab A. Ali	1
Dr. J. M. Baird	1
Dr. L. Barnett	1
Dr. O. Book	1
Dr. Jay Boris	1
Dr. K. R. Chu	1
Dr. Timothy Coffey	1
Dr. G. Cooperstein	1
Dr. A. Drobot	1
Dr. Richard Fernslor	1
Dr. H. Freund	1
Dr. M. Friedman	1
Dr. J. Golden	1
Dr. S. Goldstein	1
Dr. V. Granatstein	1
Dr. Robert Greig	1
Dr. Irving Haber	1
Dr. Richard Hubbard	1
Dr. Bertram Hui	1
Dr. Glenn Joyce	1
Dr. Selig Kainer	1
Dr. C. A. Kapetanakos	1
Dr. M. Lampe	1
Dr. Y. Y. Lau	1
Dr. W. M. Manheimer	1
Dr. Don Murphy	1
Dr. Peter Palmadesso	1
Dr. Robert Pechacek	1
Dr. Michael Picone	1
Dr. Michael Raleigh	1
Dr. M. E. Read	1
Dr. C. W. Roberson	1
Dr. J. D. Sethian	1
Dr. William Sharp	1
Dr. J. S. Silverstein	1
Dr. Philip Sprangle	1
Dr. Doug Strickland	1
Dr. C. M. Tang	1
Dr. N. Vanderplaats	1
Washington, DC 20375	

	Copies
Office of Naval Research	
Attn: Dr. Robert Behringer	1
1030 E. Green	
Pasadena, CA 91106	
Office of Naval Research	
Attn: Dr. T. Berlincourt	1
Dr. W. J. Condell	1
Department of the Navy	
Arlington, VA 22217	
Commander	
Naval Air Systems Command	
Attn: Dr. Wasneski	1
Department of the Navy	
Washington, DC 20361	
Commander	
Naval Sea Systems Command	
Attn: Dr. C. F. Sharn	1
Department of the Navy	
Washington, DC 20362	
Harry Diamond Laboratory	
Attn: Dr. H. E. Brandt	1
Dr. S. Graybill	1
2800 Powder Mill Road	
Adelphi, MD 20783	
U. S. Army Ballistic Research Laboratory	
Attn: Dr. D. Eccleshall	1
Aberdeen Proving Ground	
MD 21005	
Air Force Weapons Laboratory	
Attn: Dr. Ray Lemke	1
Kirtland Air Force Base	
Albuquerque, NM 87117	
Air Force Weapons Laboratory	
Attn: Dr. D. Straw	1
Kirtland AFB, NM 87117	

DISTRIBUTION (Cont.)

	Copies
U.S. Department of Energy	
Attn: Dr. T. Godlove	1
Dr. M. Month	1
Dr. J. A. Snow	1
Washington, DC 20545	
National Bureau of Standards	
Attn: Dr. Sam Penner	1
Bldg. 245	
Washington, DC 20234	
National Bureau of Standards	
Attn: Dr. Mark Wilson	1
Gaithersburg, MD 20760	
Defense Advanced Research Projects Agency	
Attn: Dr. J. Bayless	1
Dr. Robert Fossum	1
Dr. J. A. Mangano	1
LCOL W. Whitaker	1
1400 Wilson Blvd.	
Arlington, VA 22209	
Science Applications Inc.	
Attn: Dr. Richard E. Aamodt	1
934 Pearl St. Suite A	
Boulder, CO 80302	
Science Applications Inc.	
Attn: Dr. L. Feinstein	1
Dr. Robert Johnston	1
Dr. Douglas Keeley	1
Dr. John Siambis	1
5 Palo Alto Square	
Palo Alto, CA 94304	
Science Applications, Inc.	
Attn: Dr. A. W. Trivelpiece	1
San Diego, CA 92123	
Science Applications, Inc.	
Attn: Dr. Ron Parkinson	1
1200 Prospect Street	
P.O. Box 2351	
La Jolla, CA 92038	

	Copies
TRW	
Defense and Space Systems Group	
Attn: Dr. D. Arnush	1
Dr. M. Caponi	1
1 Space Park	
Redondo Beach, CA 90278	
Lawrence Livermore National Laboratory	
Attn: Dr. W. A. Barletta	1
Dr. R. Briggs	1
Dr. H. L. Buchanan	1
Dr. Frank Chambers	1
Dr. T. Fessenden	1
Dr. Edward P. Lee	1
Dr. James Mark	1
Dr. Jon A. Masamitsu	1
Dr. V. Kelvin Neil	1
Dr. R. Post	1
Dr. D. S. Prono	1
Dr. M. E. Rensink	1
Dr. Simon S. Yu	1
University of California	
Livermore, CA 94550	
Physics International Co.	
Attn: Dr. Jim Benford	1
Dr. S. Putnam	1
2700 Merced Street	
San Leandro, CA 94577	
Sandia Laboratories	
Attn: Dr. K. D. Bergeron	1
Dr. B. Epstein	1
Dr. S. Humphries	1
Dr. Tom Lockner	1
Dr. Bruce R. Miller	1
Dr. C. L. Olson	1
Dr. Gerold Yonas	1
Albuquerque, NM 87115	
La Jolla Institute	
Attn: Dr. K. Brueckner	1
Prof. N. M. Kroll	1
P.O. Box 1434	
La Jolla, CA 92038	

DISTRIBUTION (Cont.)

	Copies
Mission Research Corp.	
Attn: Dr. Neal Carron	1
Dr. Conrad Longmire	1
735 State Street	
Santa Barbara, CA 93102	
Mission Research Corp.	
Attn: Dr. B. Godfrey	1
1400 San Mateo Blvd, S.E.	
Suite A	
Albuquerque, NM 87108	
McDonnell Douglas Corp.	
Attn: Dr. M. Greenspan	1
Dr. J. Carl Leader	1
P. O. Box 516	
St. Louis, MO 63166	
Los Alamos National Lab.	
Attn: Dr. Barry Newberger	1
Dr. L. E. Thode	1
Mail Stop 608	
Los Alamos, NM 87544	
Los Alamos Scientific Lab.	
Attn: Dr. H. Dreicer	1
Dr. R. J. Faehl	1
Los Alamos, NM 87544	
Pulse Sciences, Inc.	
Attn: Dr. Sid Putnam	1
1615 Broadway, Suite 610	
Oakland, CA 94612	
National Science Foundation	
Attn: Dr. R. Hill	
Physics Division, #341	
Washington, DC 20550	
W. J. Schafer Associates, Inc.	
Attn: Dr. Edward Cornet	1
1901 North Fort Myer Dr.	
Arlington, VA 22209	

	Copies
Austin Research Associates	
Attn: Prof. W. E. Drummond	1
Dr. M. Lee Sloan	1
Dr. James R. Thompson	1
1901 Rutland Drive	
Austin, TX 78758	
Western Research Corporation	
Attn: Dr. Franklin Felber	1
8616 Commerce Avenue	
San Diego, CA 92121	
Jaycor	
Attn: Dr. J. U. Guillory	1
Dr. D. Tidman	1
205 S. Whiting Street	
Alexandria, VA 22304	
Varian Associates	
Attn: Dr. Howard Jory	1
611 Hansen Way	
Palo Alto, CA 94303	
Lawrence Berkeley Lab.	
Attn: Dr. Denis Keefe	1
Dr. Hogil Kim	1
Dr. Hong Chul Kim	1
Dr. Kwang Je Kim	1
Dr. L. J. Laslett	1
Dr. G. R. Lambertson	1
Dr. A. M. Sessler	1
Dr. L. Smith	1
1 Cyclotron Road	
Berkeley, CA 94720	
Stanford Linear Accelerator Center	
Attn: Dr. Philip Morton	1
P.O. Box 4349	
Stanford, CA 94305	
AVCO - Everett Research Laboratory, Inc.	
Attn: Dr. Richard Patrick	1
2385 Revere Beach Pkwy	
Everett, MA 02149	

DISTRIBUTION (Cont.)

	Copies
Oak Ridge National Lab	
Attn: Dr. J. A. Rome	1
Oak Ridge, TN 37850	
University of California at Los Angeles	
Attn: Prof. F. Chen	1
Dr. A. T. Lin	1
Dr. J. Dawson	1
Dr. C. S. Liu	1
Dr. Edward Ott	1
Los Angeles, CA 90024	
University of Maryland	
Attn: Dr. W. Destlar	1
Dr. C. S. Liu	1
Dr. Won Namkung	1
Dr. E. Ott	1
Prof. M. Reiser	1
Dr. Moon-Jhong Rhee	1
Dr. C. D. Striffler	1
College Park, MD 20742	
Columbia University	
Attn: Prof. P. Diament	1
Prof. S. Schlesinger	1
New York, NY 10027	
North Carolina State University	
Attn: Prof. W. Doggett	1
Dr. Jin Joong Kim	1
P. O. Box 5342	
Raleigh, NC 27650	
Massachusetts Institute of Technology	
Attn: Prof. George Bekefi	1
Dr. K. J. Button	1
Prof. R. Davidson	1
Dr. R. Temkin	1
77 Massachusetts Avenue	
Cambridge, MA 02139	
University of California	
Attn: Dr. Gregory Benford	1
Dr. A. Fisher	1
Prof. N. Rostoker	1
Physics Department	
Irvine, CA 92717	
Yale University	
Attn: Dr. I. B. Bernstein	1
Dr. J. L. Hirshfield	1
Mason Laboratory	
400 Temple Street	
New Haven, CT 06520	
Cornell University	
Attn: Prof. H. Fleischmann	1
Prof. D. Hammer	1
Prof. R. V. Lovelace	1
Prof. J. Nation	1
Prof. R. Sudan	1
Ithaca, NY 14850	
University of Texas at Austin	
Attn: Dr. M. N. Rosenbluth	1
Institute for Fusion Studies	
RLM 11.218	
Austin, TX 78712	
Stevens Institute of Technology	
Attn: Prof. George Schmidt	1
Physics Department	
Hoboken, NJ 07030	
Dartmouth College	
Attn: Dr. John E. Walsh	1
Department of Physics	
Hanover, NH 03755	
Defense Technical Information Center	
Cameron Station	
Alexandria, VA 22314	12


DATE
ILMED
8